Transport of Long-Chain Native Fatty Acids across Human Erythrocyte Ghost Membranes†

Alan M. Kleinfeld,* Scott Storms, and Michael Watts

Medical Biology Institute, 11077 North Torrey Pines Road, La Jolla, California 92037

Received February 5, 1998; Revised Manuscript Received March 26, 1998

ABSTRACT: Evidence from a number of laboratories suggests that membrane proteins may meditate the transport of physiologic fatty acids (FA) across cell membranes. However, actual transport of unbound free fatty acids (unbound FFA) from the aqueous phase on one side of a cell membrane to the aqueous phase on the other side has not been measured previously. In this study, we have used the fluorescent probe of unbound FFA, ADIFAB, to monitor the time course of FA movement from the outer to the inner aqueous compartments, and from the lipid membrane to the outer aqueous compartment of red cell ghosts. These two measurements, together with measurements of the lipid/aqueous partition coefficients, allowed the determination of the rate constants for binding (k_{on}), flip-flop (k_{ff}), and dissociation (k_{off}) for the transport of long-chain natural FA across red cell ghosts. Measurements done using palmitate, oleate, and linoleate at temperatures between 20 and 37 °C revealed that the overall transport times ranged from about 0.5 to more than 10 s, depending upon FA type and temperature. Analysis of these time courses yielded k_{ff} values between 0.3 and 3.0 s^{-1}, and these values were consistent with those obtained using ghosts containing pyranine to detect intracellular acidification by the translocating FA. The measured k_{off} values ranged from about 0.3 to 5 s^{-1}, while the rate of binding, for the ghost concentrations used in this study (>50 μM phospholipid), exceed both k_{ff} and k_{off}. Thus, long-chain FA transport across red cell ghost membranes is rate-limited by a combination of flip-flop and dissociation rates. Binding of FA to ghost membranes was well described by simple, nonsaturable, aqueous/membrane partition, and that partition appears to be governed by the aqueous solubility of the FA. Transport rates did not reveal any evidence of saturation and were not affected by a variety of protein-specific reagents. These FA binding and transport characteristics are similar to those observed previously for lipid vesicles, although the rate constants are generally about 2−3 fold larger for ghosts as compared to the lipid vesicles. We suggest, therefore, that FA transport across red cell ghosts is reasonably well described by transport across the lipid phase of the membrane.

Determining how fatty acids (FA)[1] are transported across cell membranes is important for understanding the physiology of FA utilization. Transport across membranes involves (1) desolvation of the FA from the aqueous phase and insertion into the outer hemileaflet of the membrane (k_{on}), (2) translocation or flip-flop from one hemileaflet to the other (k_{ff}), and (3) dissociation from the inner hemileaflet into the aqueous phase (k_{off}). Studies in bacteria, yeast, and a variety of mammalian cells have obtained evidence that one or more of these steps is protein-mediated (*1*−*12*). In contrast with these results, evidence from a number of laboratories is consistent with a mechanism in which FA transport across cell membranes occurs by diffusion through the lipid phase of the membrane (*13*−*18*). It is implicit in a protein-facilitated process that FA transport through the lipid phase of the membrane does not occur at a rate sufficient to support the level of FA metabolism required by the cell. Most studies in lipid vesicles indicate that FAs can spontaneously cross lipid membranes (*17*, *19*−*24*). However, at issue even for these simplest of membranes is the identity and magnitude of the rate-limiting step for transport across lipid membranes; if this rate is greater than required for cellular metabolism, then a protein-facilitated mechanism might not be needed.

Actual transport of FA between the aqueous phases on either side of a cellular membrane has not been measured previously because the low solubility of the long-chain FA prevented the detection of the aqueous phase concentration of FA with sufficient sensitivity and temporal resolution. This limitation can now be overcome using the fluorescent probe ADIFAB which can determine the unbound free fatty acid (unbound FFA),[2] or aqueous phase, concentration with nanomolar accuracy and millisecond resolution (*25*, *26*). Recently, we have used ADIFAB to study long-chain FA transport across lipid vesicle membranes, and these studies revealed that flip-flop is rate-limiting at least for transport across lipid bilayer vesicles of diameters ≥1000 Å (*27*).

† This work was supported by Grant GM44171 from the National Institute of General Medical Sciences.

* To whom correspondence should be addressed.

[1] Abbreviations: ADIFAB, rat intestinal fatty acid binding protein labeled at Lys^{27} with acrylodan; FA, fatty acid; FAFBSA, fatty acid free BSA; LA, linoleate (18:2); OA, oleate (18:1); PA, palmitate (16:0); unbound FFA, unbound free fatty acid.

[2] The aqueous phase concentration of fatty acid monomers is designated here as unbound free fatty acids (unbound FFA). In many of our previous publications (*25*−*27*, *41*, *43*−*47*) we have referred to these same molecules simply as free fatty acids (FFA).

S0006-2960(98)00301-8 CCC: $15.00
Published on Web 05/12/1998

Moreover, these studies indicate that the rate of flip-flop is quite sensitive to the diameter and composition of the bilayer, raising the possibility that transport through the lipid phase of a cell membrane might not be sufficient to support metabolic rates, at least in cells for which high levels of FA transport are important.

This new technology should also be applicable to measurements of actual FA transport across cell membranes, and this should, preferably, be done in cells for which FA metabolism plays an important role. However, because of the lack of consensus about these more complex systems, we have chosen to address this issue initially in human red cell ghosts, among the simplest and best characterized biological membranes. Although FA transport is not central to red cell physiology, erythrocytes possess an ATP-driven acyl-CoA transferase that requires transmembrane transport of long-chain FA (*28*). Previous studies in red cells have reported quite different rates and mechanisms of FA transport (*29*−*36*). In particular, transport may be energy-dependent (*29*), mediated by "protein-determined lipid micro domains" but probably not energy-dependent (*32*−*36*), and probably not protein-mediated (*31*). Transport of unbound FFA, defined as movement of unbound FFA between aqueous phases on either side of the membrane, was not measured in these studies. Rather, the transport mechanism and rates were inferred from the kinetics of radiolabeled FA uptake and extraction from intact red cells and ghosts.

In the present study, we have used ADIFAB to monitor the transport of FA both from the outside to the inside of human red cell ghosts with ADIFAB trapped inside and from the ghosts to extracellular ADIFAB, to determine the dissociation rate constants. These measurements together with the determination of the aqueous/membrane partition coefficients allowed us to determine all three of the rate constants (k_{on}, k_{ff}, k_{off}) that characterize transport across the membranes. We also trapped in ghosts the fluorescent pH indicator pyranine, and used these membranes to provide an independent determination of the flip-flop times. Our results for palmitate, oleate, and linoleate demonstrate that transport across red cell ghosts requires times of from 0.5 to more than 10 s, depending upon the FA type and temperature. In all cases, the rate of flip-flop is less than or equal to the rate of dissociation, indicating that these two processes in combination represent the rate-limiting step for transport across red cell ghosts membranes. The transport time courses are not affected by protein modification or the concentration of unbound FFA. Moreover, the FA binding and transport characteristics for ghosts are similar to those for 2000 Å diameter lipid vesicles composed of egg phosphatidylcholine and cholesterol determined previously, although 2−3-fold larger than for the lipid vesicles (*27*), suggesting that transport across red cell ghost membranes is not protein-mediated.

METHODS

Materials. Pyranine (8-hydroxyprene-1,3,6-trisulfonic acid), DIDS (4,4′-diisothiocyanatostilbene-2,2′-disulfonic acid), and H_2-DIDS (4,4′-diisothiocyanatodihydrostilbene-2,2′-disulfonic acid were purchased from Molecular Probes (Eugene, OR). ADIFAB was prepared as described (*25*) and is available from Molecular Probes. For all measurements, the sodium salts of the FA (Nu Chek Prep, Elysian, MN) were used, as described previously (*25*). Stock solutions of the FA salt were prepared in 20 mM KOH and were maintained under argon at −20 °C. The buffer (buffer A) used to measure FA transport, dissociation, and binding with ADIFAB consisted of 20 mM HEPES, 126 mM NaCl, and 6 mM $MgCl_2$ at pH 7.4, unless otherwise stated. Essentially fatty acid free bovine serum albumin (BSA), chymotrypsin, iodoacetamide, papain, and trypsin were purchased Sigma (St. Louis, MO). High-purity BSA (True Chon Crystalline) was purchased from ICN (Costa Mesa, CA), and *N*-ethylmaleimide (NEM) was purchased from Eastman (Rochester, NY).

Preparation of Red Cell Ghosts. In- and out-dated red cells and/or whole blood was obtained from the San Diego Blood Bank, and the preparation of ghosts was based upon that described in (*37*, *38*). Unless indicated otherwise, all preparations were done on ice or at 4 °C. Cells were washed 3 times in isotonic buffer, and the buffy coat was carefully removed after each wash. Red cells at 50% hematocrit were lysed by a 30-fold dilution in 10 mM HEPES at pH 7.4 (lysing buffer), and these lysed cells were centrifuged at 10000*g* for 40 min. This procedure produces pink ghosts, and white ghosts are prepared by repeating the lysis steps 4 times. Ghosts were sealed with or without ADIFAB or pyranine trapped inside by mixing packed ghosts (by centrifugation at 14 000 rpm in an Eppendorf centrifuge for 10 min) with up to 1 mM ADIFAB or 1 mM pyranine in lysing buffer and incubating for about 30 min. Sealing was initiated by adding salts and HEPES, incubating under argon for 1 h at 37 °C, and centrifuging at 14 000 rpm (Eppendorf) for 10 min. Unless stated otherwise, the ghost dispersion was buffered in 20 mM HEPES, 126 mM NaCl, and 6 mM $MgCl_2$ at pH 7.4 (buffer A). The pellet was applied to a dextran gradient consisting of three densities of 2.06 g, 3.44 g, and 4.80 g per 25 mL and was centrifuged for 3 h at 25 000 rpm in a Sorvall AH-627 swinging-bucket rotor. Generally, more than 90% of the pink and less than 50% of the white ghosts were sealed (float at the first water/dextran water interface); unsealed ghosts appear at the bottom of the gradient. Sealed ghosts were washed, stored under argon at 4 °C, and generally used within 2 days. The concentration of ADIFAB in sealed ghosts was between 60 and 200 μM. Although the ghosts are sealed when collected at the water/dextran interface, it was necessary to determine (a) whether ADIFAB and pyranine were trapped in the inner aqueous phase rather than absorbed to the outer hemileaflet and (b) whether the ghosts remained intact during stopped-flow mixing. To do this, we assayed for the accessibility of ADIFAB and pyranine to the fluorescence quenchers sodium molybdate and $CoCl_2$, respectively, as described previously (*27*). Throughout this study, selected samples of the sealed ghost preparation were examined by light microscopy (both transmitted and fluorescence from samples with trapped ADIFAB and pyranine), and all exhibited normal biconcave shape. The concentration of ghost membrane was determined by tryptophan fluorescence and phospholipid concentration by assaying for inorganic phosphate (*39*), and unless stated otherwise, ghost concentrations are reported as molar phospholipid.

Endogenous FA. As a consequence of either endogenous lipase or autohydrolytic activity, the final ghost preparation exhibited varying levels of FA, as detected by ADIFAB. In

some instances, endogenous FA levels were sufficiently high to interfere with transport or dissociation time courses of the exogenous FA. Thus, before adding FA we routinely measured the time course of fluorescence from ghosts with trapped ADIFAB or pyranine that were stopped-flow-mixed with fatty acid free BSA (FAFBSA), and the time course of sealed ghosts mixed with ADIFAB, to assess the influence of endogenous FA on transport and dissociation measurements, respectively. FA was extracted from preparations with high levels of endogenous FA by incubation for 1 h at room temperature or overnight at 4 °C with 200−400 μM FAFBSA, followed by extensive washing to remove BSA.

Protein Modifications. Red cells and ghosts were treated with proteases and specific protein reagents to modify free SH groups (NEM and iodoacetamide) and NH groups (DIDS and H_2DIDS). Ghosts or intact red cells were treated with chymotrypsin, papain, Pronase, or trypsin, by incubating ghosts or cells with (1−2 mg/mL) enzyme in 145 mM KCl, 10 mM $NaHPO_4$, pH 7 (buffer B), for times between 1 and 3 h at 37 °C. Cells or ghosts (50 μM) were reacted with DIDS or H_2DIDS (1−50 μM) in buffer B at pH 8 for 3 h at 37 °C. For reactions with NEM and iodoacetamide, 2 mM reagent and 400 μM ghosts/cells were incubated for 2 h at 37 °C in buffer A and buffer B at pH 9, respectively. Following reactions with all reagents, ghosts/cells were washed and resuspended in buffer A.

Fatty Acid Addition. FA were stopped-flow-mixed either in the absence or as a complex with BSA. Without BSA present, solutions of unbound FFA were prepared at pH ∼10 using a buffer consisting of 1 mM HEPES and isotonic NaCl which when mixed with the ghost buffer A yielded a final pH of 7.4, as described previously (*23*). The concentration of unbound FFA in this solution was less than the solubility limit of each FA at pH 7.4: about 6 μM for PA and OA, and 15 μM for LA (*25*). Adding unbound FFA in this way presents the ghosts with initial unbound FFA concentrations that exceed physiologic levels by more than 1000-fold (*40*). Frequently, this method of mixing unbound FFA and ghosts resulted in lysis during stopped-flow (data not shown). We found previously that certain lipid vesicles also revealed a loss of integrity during stopped-flow mixing. We speculated that this might be a consequence of the sudden transmembrane asymmetry of FA that develops shortly after stopped-flow mixing when these high concentrations of unbound FFA partition rapidly into the outer hemileaflet of the membrane (*27*).

By adding unbound FFA using FA−BSA complexes, the unbound FFA concentration remains constant and 10−1000-fold lower than without BSA. This eliminates the potentially large transmembrane FA gradient that may occur immediately after stopped-flow mixing and yields conditions that more accurately simulate physiology. Most of the transport studies, therefore, were done by adding unbound FFA using FA−BSA complexes. These complexes were prepared by titrating, at 37 °C, a solution of BSA with FA, so that the unbound FFA concentration of each aliquot was less than the solubility limit for the FA at pH 7.4. During and after the titration, unbound FFA levels were measured using ADIFAB as described previously (*25*, *41*). The complexes were used at BSA concentrations sufficient to buffer the unbound FFA levels in the presence of the ghosts, and these levels were determined by direct measurement of the unbound FFA level in the suspension of ghosts and FA−BSA complexes. For the concentrations of ghosts used in these studies (∼50 μM), 50 μM BSA was sufficient to buffer unbound FFA levels even for relatively high FA:BSA ratios (>4:1). Under these conditions, the fraction of FA that is transferred from BSA to the ghost membranes is less than 2%.[3] The rate of FA dissociation from BSA is not expected to be rate-limiting for this amount of FA transferred, because the dissociation rate constant for oleate at 37 °C is 0.16 s^{-1} (*42*) and therefore 2% of the bound FA should dissociate in <130 ms.

Fluorescence Instrumentation. Steady-state fluorescence measurements were done using either an SLM 4800 or an SLM 8100 fluorometer. ADIFAB fluorescence was excited at 386 nm; excitation and emission were monitored at 505 and 432 nm. Pyranine was excited at 455 nm, and emission was monitored at 509 nm. Most of the stopped-flow fluorescence was measured using a KinTek Instrument (State College, PA) in which two equal volumes (about 0.1 mL) of reactants were mixed at 1 mL/s with a dead time of <5 ms as described previously (*43*). Stopped-flow fluorescence was measured using two photomultipliers placed on opposite sides of the viewing chamber, and intensities were monitored through 20 nm bandwidth filters centered at 432 and 505 nm (Omega Optical, Brattleboro, VT). A minimum of 5 scans were acquired for each condition, and 500 data points were collected per scan.

FA/Membrane Partition Coefficients. Coefficients of FA partition (K_p) between buffer and red cells were determined as described previously (*44*, *45*). Briefly, FA were added to a solution containing 0.5−1 μM ADIFAB plus 50−100 μM ghosts, incubated for 10 min, and [unbound FFA] was determined from the ratio of the ADIFAB fluorescence emission intensities at 505 to 432 nm (R value). These measurements were done for temperatures between 20 and 40 °C, and at each temperature, FA were added to give total FA to phospholipid mole ratios that ranged from 3 to 40%. The partition coefficient was computed as $K_p = (([FA_T] - [\text{unbound FFA}])/[\text{unbound FFA}])V_a/V_m$, where $[FA_T]$ is the total FA concentration in the cuvette and V_a and V_m are the volumes of aqueous and membrane phases, respectively, and a value of 10^6/M phospholipid was used for V_m/V_a (*44*). Measurements were done for laurate, myristate, palmitate, oleate, linoleate, linolenate, and arachidonate and revealed that K_p values increased with decreasing aqueous solubility of the FA so that linolenate has the lowest (2×10^4) and palmitate, at 8×10^5, the highest K_p value (Table 1). Moreover, K_p values were independent of both the mole ratio of FA and the temperature (data not shown). Both the magnitudes as well as the lack of concentration and temperature dependence of the K_p values obtained in ghosts are consistent with the values reported previously for lipid vesicles and murine tumor cells (*44*, *45*).

[3] For a given [unbound FFA], the concentration of FA that partitions into the ghost membranes is given by $[FA_m] = [\text{unbound FFA}]\ V_a/V_m$ where V_a and V_m are defined in the section on partition. This is the concentration of FA that is transferred from the FA−BSA complex. Typically, the ghost concentration is 50 μM phospholipid, and with unbound oleate equal to 200 nM, the concentration of oleate that partitions into the membrane ($K_p = 4 \times 10^5$) is about 5 μM. For 50 μM BSA and a OA:BSA ratio > 4:1 (needed to generate 200 nM), 5 μM represents <2% of the total FA of the oleate−BSA complex.

Table 1: Coefficients of FA Partition between Red Cell Ghost Membranes and Aqueous Media[a]

fatty acid	partition coefficient ($\times 10^{-4}$)	fatty acid	partition coefficient ($\times 10^{-4}$)
LAU	2	LA	13
MA	4	LNA	2
PA	80	AA	12
OA	40		

[a] These K_p values were determined in buffer A as described under Methods. For each FA, at least four different concentrations were used so that the mole percent FA relative to the phospholipid concentration of the ghosts ranged from about 3 to 40%. K_p values were invariant with FA concentration, and therefore the values listed in the table are the averages over all concentrations. Measurements were done at temperatures between 20 and 40 °C except for LAU, MA, and LNA, for which values only at 25 °C were determined. No significant variation with temperature was observed for PA, OA, LA, and AA so that the values for these FA are also averaged over all temperatures. Uncertainties from multiple determinations were about 20%. FA are abbreviated as follows: AA, arachidonate; LA, linoleate; LAU, laurate; MA, myristate; LNA, linolenate; OA, oleate; PA, palmitate.

Determination of Rate Constants for FA Dissociating from, Transferring across, and Binding to Red Cell Ghosts. To determine the rate constants (k_{off}, k_{ff}, k_{on},) that characterize FA transport across the membranes, time courses of FA movement, corresponding to different arrangements of FA, ghosts, and ADIFAB, were analyzed using the kinetic models described previously for lipid vesicles (*27*). The measurements of FA dissociation from ghosts to ADIFAB were analyzed to yield k_{off} values, and k_{on} was calculated as $k_{on} = K_p k_{off}$. Transport time courses were analyzed to determine k_{ff} as previously when FA were added without BSA. For the transport measurements in which FA were added as complexes with BSA, this previous kinetic model could be simplified because the extracellular unbound FFA concentration (unbound FFA_o) is constant, and the equations that apply in this case are

$$\frac{d[FAm_o]}{dt} = -k_{off}[FAm_o] + k_{on}[L][FFA_o] + k_{ff}([FAm_i] - [FAm_o]) \quad (1)$$

$$\frac{d[FAm_i]}{dt} = k_{ff}([FAm_o] - [FAm_i]) - k_{off}[FAm_i] + k_{on}[L][FFA_i] \quad (2)$$

$$\frac{d[FFA_i]}{dt} = k_{off}[FAm_i] - k_{on}[L][FFA_i] \quad (3)$$

$[FAm_{o,i}]$ are the concentrations of FA in the outer and inner leaflet of the bilayer, respectively, $[FFA_{i,o}]$ are the unbound FFA concentrations inside and outside the ghosts, and [L] is the lipid concentration of the ghosts. As in our previous studies, the program MLAB (Civilized Software, Bethesda, MD) was use to carry out the least-squares fits of the solutions of these kinetic models to the measured time courses. In our analysis of the transport time courses, we often observed improvement in the quality of the fits by allowing k_{off} to exceed (by 2−10-fold) the value determined from the dissociation measurements. We speculate that this could be due to an effective intracellular off rate constant that is larger than k_{off}, which might occur because intracellular ADIFAB, on average, probes distances closer to the membrane than in the extracellular case. Single exponential fits were applied to the pyranine time course to obtain the time constants for acidification rather than k_{ff} values, as described previously (*27*).

RESULTS

Transport of Long-Chain FA across Red Cell Ghosts. Transport of long-chain FA from the external aqueous phase into the inner aqueous phase was measured by stopped-flow mixing of FA with red cell ghosts containing trapped ADIFAB. The ratio of ADIFAB fluorescence intensities at 505 and 432 nm [$R(t)$] provides a direct measure of the concentration of unbound FFA ([unbound FFA_i]) in the internal aqueous compartment of the ghosts (*25*, *27*). Results of these transport measurements reveal that $R(t)$ increases, after mixing, from an initial value R_o and approaches equilibrium at between 1 and 20 s, depending upon FA type and temperature (Figure 1). At equilibrium, the value determined for [unbound FFA_i] was equal to the concentration of extracellular unbound FFA ([unbound FFA_o]). The results show that transport rates are smallest for palmitate (16:0) and oleate (18:1) which are about 30% that of linoleate (18:2). Transport rates also increase with temperature, roughly 2-fold between 20 and 37 °C, for all three FA. Rates were virtually independent of the [unbound FFA_o] for initial concentrations that ranged, for example, in the case of oleate, from about 5 nM to greater than 3000 nM (Figure 2), and similar characteristics were observed for palmitate and linoleate. Thus, for unbound FFA concentrations well within the normal physiologic range of 7 nM (*40*) to values that are more than 100-fold greater, rates of FA transport across red cell ghosts do not exhibit saturation. Similar rates and transport characteristics were found for pink or white ghosts prepared from freshly drawn, in-dated or out-dated blood (data not show).

The Ghost Membrane Is the Rate-Limiting Barrier for FA Transport. The results in Figure 1 were obtained by adding the FA in complex with BSA. This allows the FA−BSA complex to deliver sufficient amounts of FA while maintaining unbound FFA_o at low levels. Because FA must first dissociate from BSA before being transported, dissociation from BSA, rather than transport across the membrane, might be the rate-limiting step observed in the transport results of Figure 1. Although, as discussed under Methods, the rate of FA dissociation from BSA is not expected to be rate-limiting, we investigated this directly by measuring transport in lysed ghosts and lipid vesicles, and in intact ghosts using FA that was not complexed with BSA. The time course, when FA is added in complex with BSA to lysed ghosts, peaks in less than 200 ms and then decays to equilibrium in less than 500 ms (Figure 3). In contrast, the time course for intact ghosts exhibits the slow (>5 s) monotonic approach to equilibrium described in Figure 1. The rapid increase in $R(t)$ observed for lysed ghosts reflects the rapid binding of FA to ADIFAB followed by a slower decay toward equilibrium as FA dissociates from ADIFAB and partitions into the membrane, as discussed previously for lipid vesicles (*27*). Further support that dissociation from BSA is not rate-limiting are the results of measurements done by adding FA without complexing with BSA at low enough concentrations so that at least some ghost preparations are not lysed.

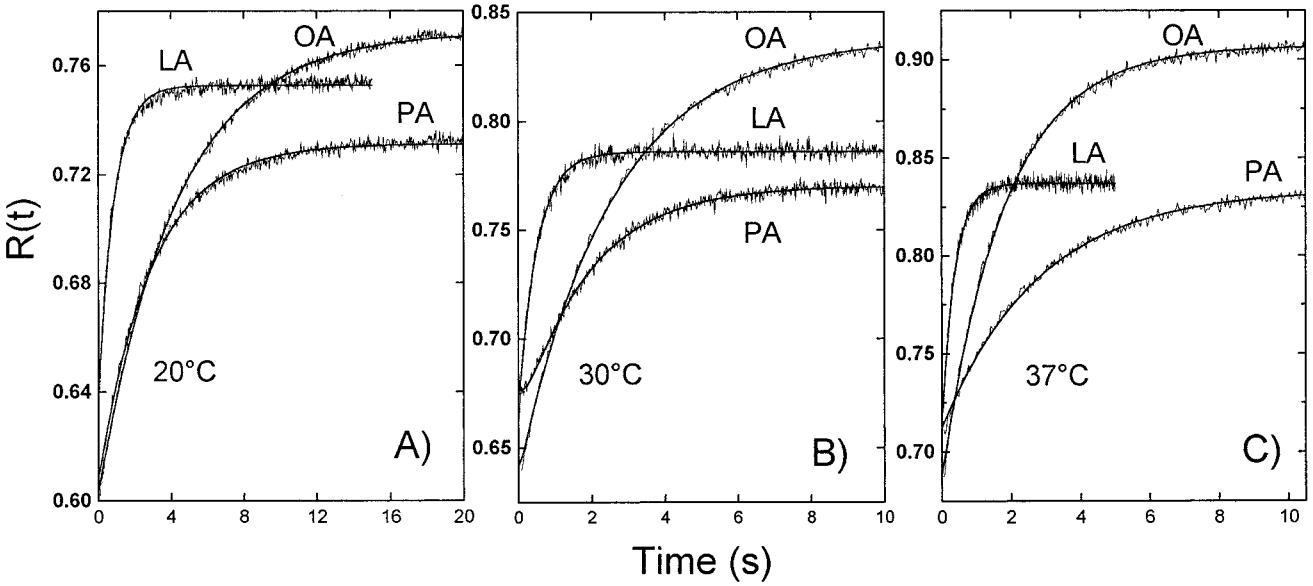

FIGURE 1: Transport of FA across red cell ghosts. Time courses of the 505 to 432 nm ratio of ADIFAB fluorescence intensities [$R(t)$] following stopped-flow mixing of red cell ghosts (25 μM) containing ADIFAB (400 μM) with FA−BSA (25 μM) complexes. Measurements were done at temperatures of 20, 30, and 37 °C, and each trace is an average of more than five individual time courses. The solid lines through the data are best fits using $R(t)$ calculated with solutions to eqs 1−3, as described under Methods. (A) Results for palmitate, oleate, and linoleate at 20 °C were obtained with unbound FFA concentrations (nM) of 72, 66, and 133, respectively, for which fit results yielded k_{ff} values (s^{-1}) of 0.4, 0.28, and 1.5, respectively. (B) Results at 30 °C were obtained with unbound FFA concentrations (nM) of 14, 87, and 190, respectively, for which fit results yielded k_{ff} values (s^{-1}) of 0.45, 0.46, and 3.0, respectively. (C) Results at 37 °C were obtained with unbound FFA concentrations (nM) of 72, 107, and 194, respectively, for which fit results yielded k_{ff} values (s^{-1}) of 0.4, 0.6, and 4.1, respectively. All concentrations quoted here and in the other figure legends are the values obtained after mixing in the stopped-flow observation chamber. FA abbreviations are those used in Table 1.

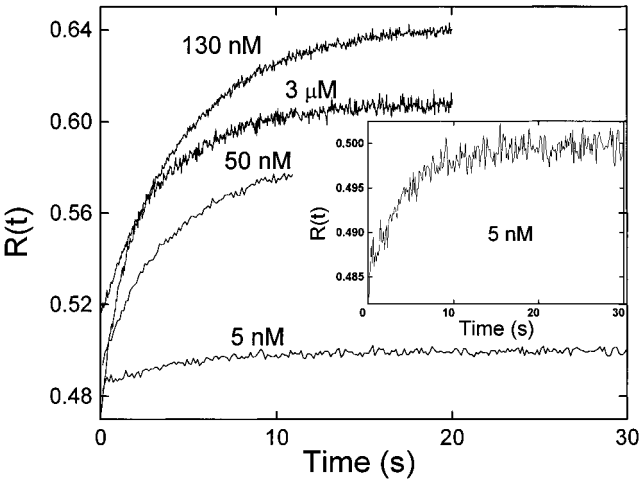

FIGURE 2: Transport of FA across red cell ghosts is independent of the unbound FFA concentration. Transport time courses at 20 °C for red cell ghosts were measured after stopped-flow mixing ghosts with increasing concentrations of unbound oleate as indicated in the figure. Unbound concentrations of 5, 50, and 130 nM were generated by mixing 50 μM ghosts with 25 μM oleate−BSA complexes of increasing oleate to BSA ratios. In addition, transport was also measured by mixing ghosts with 1 μM oleate uncomplexed with BSA. For FA added as complexes with BSA, the equilibrium values of [unbound FFA_i] are equal to the initial extracellular values ([unbound FFA_o]) whereas for uncomplexed FA, unbound FFA_o is about 60-fold greater than the equilibrium value. Rise time constants for all four concentrations are similar (~3 s), and analysis using the kinetic models for transport yields k_{ff} values between 0.2 and 0.3 s^{-1}. The insert shows an amplified view of the 5 nM trace.

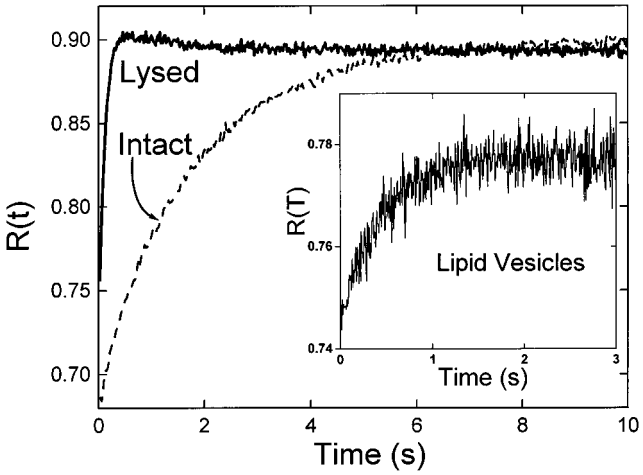

FIGURE 3: Ghost membrane is the barrier to FA transport. Time courses following stopped-flow mixing of red cell ghosts (50 μM) either osmotically lysed or intact with OA−BSA complexes (50 μM BSA), at 37 °C. Analysis of transport through the intact ghosts yields k_{ff} = 0.7 s^{-1}. Results shown in the insert are for egg phosphatidylcholine vesicles prepared, as described previously (27), by detergent dialysis and trapped with ADIFAB. These vesicles (100 μM) were stopped-flow-mixed with OA−BSA (50 μM BSA) at 20 °C and yield a rate constant of about 2 s^{-1}, about 3-fold larger than for ghosts at 37 °C. Vesicles without cholesterol exhibit much faster transport rates than vesicles containing egg phosphatidylcholine:cholesterol ≤ 3:1 (*27*).

Transport time courses from these measurements (Figure 2) are in good agreement with those obtained with FA−BSA complexes. Moreover, time courses for transport into egg phosphatidylcholine vesicles measured with FA−BSA complexes reveal rates that are about 5-fold faster than for ghosts (Figure 3). Thus, these results together with the expected times of dissociation based upon the measured rate constants (Methods) indicate that dissociation from BSA is not rate-limiting. Transport is also not rate limited by the effects of an unstirred layer (*34*) because transport rates (a) depend upon the type of FA, (b) are independent of the method of

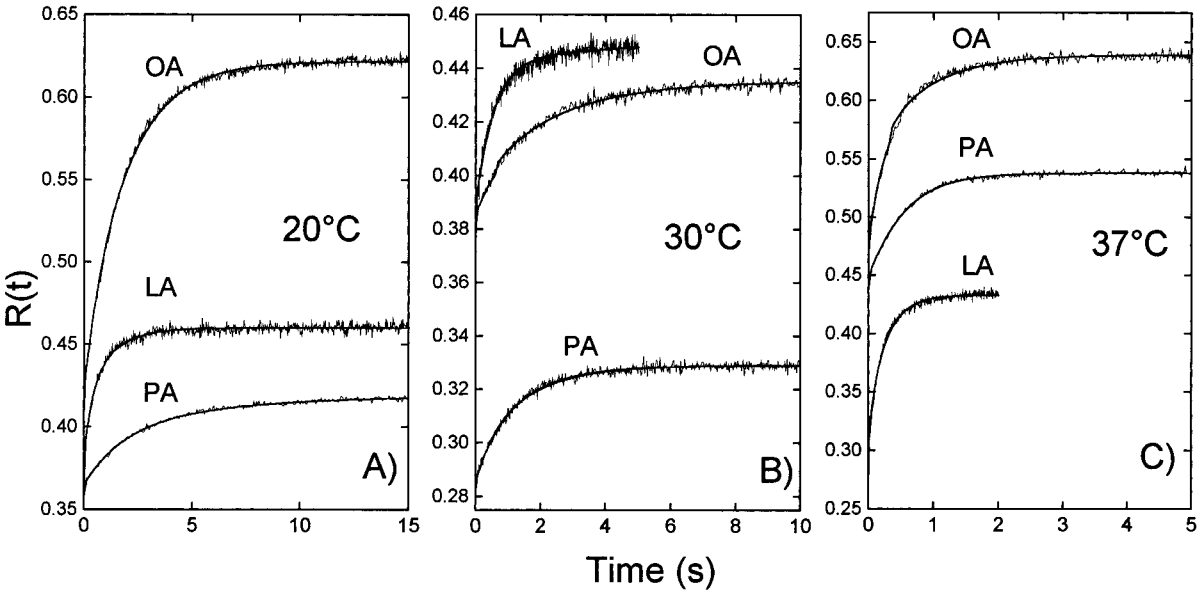

FIGURE 4: Time courses for FA dissociation from red cell ghosts. Time courses for FA dissociation from red cell ghosts following stopped-flow mixing of FA−ghost complexes with ADIFAB. Ghosts at 50 μM were incubated with 5 μM FA and mixed with 5 μM ADIFAB. The solid lines through the data are fits using the solutions to the kinetic equations for dissociation from membranes as described previously (*27*). Measurements are shown for palmitate, oleate, and linoleate at 20, 30, and 37 °C. (A) Results at 20 °C yield k_{off} values of 0.4, 0.8, and 1.4 for palmitate, oleate, and linoleate, respectively. (B) Results at 30 °C yield k_{off} values of 1.1, 0.8, and 2.3 for palmitate, oleate, and linoleate, respectively. (C) Results at 37 °C yield k_{off} values of 1, 1.8, and 5 for palmitate, oleate, and linoleate, respectively. FA abbreviations are those used in Table 1.

FA addition, and (c) are independent of the concentration of BSA (data not shown). The results described in this section indicate, therefore, that the observed time courses of transport are rate limited by transport across the ghost membrane.

Rate-Limiting Steps for Long-Chain FA Transport across Red Cell Membranes. Although these studies indicate that transport is rate-limited by the membrane and requires times of the order of seconds, they do not by themselves indicate which of the three kinetic steps is rate-limiting. Elucidation of the three rate constants that govern transport was done by determining k_{ff} from the transport time courses, after separately determining k_{off} and k_{on}, as described previously for lipid vesicles (*27*).[4] The k_{off} values were obtained from measurements of FA transfer from ghosts to extravesicular ADIFAB, using the kinetic model described previously to analyze the time courses (*27*). Results typical of these measurements are shown in Figure 4 and the analysis is represented as the solid lines through these data. Results of these measurements reveal faster rates of transfer for linoleate than for oleate and palmitate, and for all three FA, rates increase about 2-fold between 20 and 37 °C (Figure 4). Rate constants obtained from these measurements range from about 0.3 to 5 s^{-1}, depending upon temperature, FA type, and vesicle composition (Table 2). The k_{on} values (K_p/k_{off}) were calculated using the K_p values of Table 1 and the k_{off} values of Table 2, and these rate constants were found to range from about 1×10^5 M^{-1} s^{-1} for oleate at 20 °C to about 1×10^6 M^{-1} s^{-1} for linoleate at 37 °C (Table 3). These values predict rates of FA binding to 50 μM ghost membranes, for temperatures between 20 and 37 °C, that range from about 9 to 32 s^{-1} for linoleate and from 7.5 to 18 s^{-1} for palmitate, well in excess of their respective transport rates.

Flip-flop rate constants (k_{ff}) were determined by analyzing transport time courses using the k_{off} and k_{on} values of Tables 2 and 3, and representative fits of the kinetic models are

Table 2: Rate Constants for FA Dissociation from Red Cell Ghosts[a]

fatty acid	20 °C	30 °C	37 °C
oleate	0.8	0.7	2.0
palmitate	0.3	0.6	0.7
linoleate	1.4	3.0	5.0

[a] k_{off} are in units of s^{-1}. Measurements of the time course of dissociation were done for 2 to 4 different ADIFAB concentrations for each ghost preparation, and for each condition of this table, measurements were done using between three and eight different ghost preparations. The k_{off} values determined from the analysis (for example, Figure 4) of each of the separate time courses (which are each averages of at least five separate traces) were averaged, and the standard deviation of the distribution of k_{off} values for each entry in the table was about 30%.

Table 3: Rate Constants (k_{on}) for FA Binding to Red Cell Ghosts[a]

fatty acid	20 °C	30 °C	37 °C
oleate	3	3	8
palmitate	2	5	6
linoleate	2	4	7

[a] Values were calculated as $k_{on} = k_{off}K_p$ using the k_{off} values of Table 2 and the K_p values of Table 1, and are in units of 1×10^{-5} M^{-1} s^{-1}. The uncertainties in these values (SD) are about 40%, estimated using the 20% and 30% uncertainties for K_p (Table 1) and k_{off} (Table 2), respectively.

[4] Given the asymmetry of the ghost membranes, k_{off} values from the outer and inner leaflets may not be the same. The combined measurements of transport, of flip-flop by pyranine, and of dissociation from unsealed ghosts indicate that k_{off}(inside) cannot be significantly smaller than k_{off}(outside). However, the value of k_{off}(inside) may be greater than k_{off}(outside). Indeed, the quality of fits to the transport time courses was often improved by allowing k_{off} to exceed the measured value (Methods). A larger value for k_{off}(inside) than is measured for dissociation from the outer leaflet would not change significantly the derived k_{ff} values.

Table 4: Flip-Flop Rate Constants for FA Transport across Red Cell Ghosts[a]

fatty acid	20 °C	30 °C	37 °C
oleate	0.3	0.5	0.7
palmitate	0.3	0.6	0.6
linoleate	1.4	2.	3.0

[a] Values for k_{ff} are in units of s^{-1}. Transport time courses were measured for between three and seven different ghost preparations. For each preparation, a minimum of 5 separate stopped-flow traces were averaged to obtain a time course for analysis, and between 3 and more than 40 independent time courses were used to obtain k_{ff} values for the 9 different conditions of this table. The values given in the table are the averages of these independent determinations, and the standard deviation estimated from these multiple determinations was about 20%.

shown as solid lines through the data of Figures 1 and 2. The results of these analyses indicate that the k_{ff} range from about 0.3 s^{-1} for palmitate and oleate at 20 °C to about 3 s^{-1} for linoleate at 37 °C (Table 4). Thus, k_{ff} values for linoleate are about 3−4-fold greater than for palmitate and oleate, and for all three FA, k_{ff} values increase about 2-fold between 20 and 37 °C (Table 4). Moreover, we found that rates of FA dissociation were smaller from sealed than unsealed ghosts, for which the slower flip-flop process is bypassed, providing further evidence that $k_{ff} < k_{off}$ (data not shown). We conclude, therefore, that the flip-flop step is rate-limiting but that dissociation from the membrane may also contribute to the observed overall transport time courses.

FA Flip-Flop Determined by Quenching of Pyranine Fluorescence. To provide an independent determination of the FA flip-flop rates, we also used pyranine trapped within the ghosts to detect the decrease in intracellular pH as the neutral FA moves from the outer to the inner hemileaflet of the membrane (*17*, *23*). Pyranine fluorescence is quenched with decreasing pH, and the time courses following stopped-flow mixing of pyranine/ghosts with FA reveal decays which are consistent with the flip-flop rates determined using ADIFAB (Figure 5). The time course of pyranine fluorescence in lipid vesicles is well described by a monotonic decay (*23*, *27*). In contrast, pyranine fluorescence in ghosts reveals a relatively slow increase following the initial decay (Figure 5). This realkalization, which probably represents H^+/OH^- leakage, helps to limit the degree of acidification which is generally less than expected from the buffer capacity and amount of FA added. Restricting the analysis to the decay portion of the time courses, we find time constants at 37 °C that are about 3 s for oleate and palmitate and about 1 s for linoleate, and these times are about 2-fold longer at 20 °C (data not shown). Thus, the pyranine results are consistent with the flip-flop rate constants of Table 4.

Lack of Effect of Protein Modification on FA Transport across Red Cell Ghosts. In preliminary studies, we reported that treatment of ghosts with DIDS or H_2DIDS reduced the rate of FA transport into red cell ghosts, as measured by ADIFAB fluorescence (*46*, *47*). Subsequent investigations now indicate that DIDS and H_2DIDS permeate sealed ghosts and react efficiently with ADIFAB within the ghost (although not in free solution), and this reaction reduces the rate at which ADIFAB responds to FA (data not shown). Consistent with these results, ghosts prepared from intact red cells that were treated with DIDS or H_2DIDS revealed no alteration in FA transport properties. Treatment of ghosts with chymotrypsin, papain, Pronase, or trypsin also has no significant effect on FA transport rates. Finally, treatment of ghosts with the sulfhydryl reagents NEM or iodoacetamide also had no effect on transport. Thus, we conclude that transport of long-chain FA across red cell ghosts is not sensitive to protein modification, at least not by these reagents.

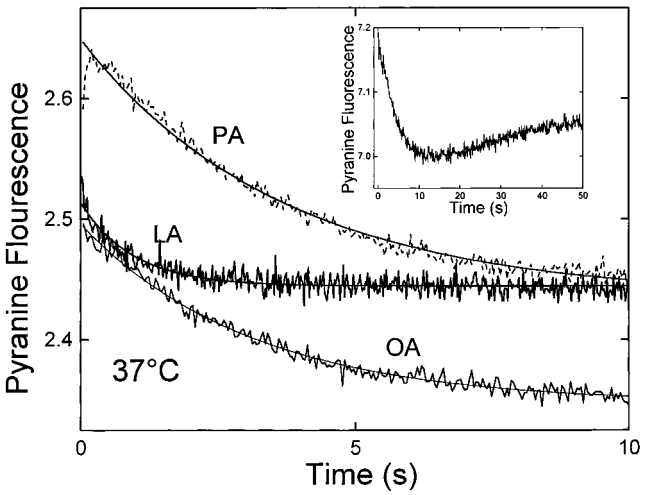

FIGURE 5: Time courses of FA-mediated quenching of pyranine fluorescence in red cell ghosts. Red cell ghosts (50 μM) with trapped pyranine, in a 5 mM HEPES buffer at pH 7.4, were stopped-flow-mixed with FA−BSA complexes for which the unbound concentrations were 200 nM for oleate and palmitate and 300 nM for linolenate. The solid curves through the data are single-exponential fits, which yield the following time constants: oleate, 3.0 s; palmitate, 2.9 s; linoleate, 1.1 s. FA abbreviations are those used in Table 1. The insert shows the alkalization that is generally observed at times longer than the more rapid FA (in this case oleate)-induced acidification.

DISCUSSION

In this study, we measured the time course for transport of long-chain FA across red cell membranes. These measurements were done using ADIFAB, the fluorescent probe of free fatty acids, to detect the transport of FA from outside to inside of the cell membranes. As far as we are aware, this report represents the first measurements of the actual transport of long-chain FA across cell membranes. The results of this study indicate that the transport of palmitate, oleate, and linoleate across red cell ghost membranes requires times of between 1 and 20 s. Transport is rate-limited by flip-flop and to a lesser extent by dissociation. The transport characteristics of red cell ghosts are similar to those reported previously for lipid vesicles composed of egg phosphatidylcholine and cholesterol with diameters ≥2000 Å (*27*). Transport across the ghost membranes does not exhibit saturation and is insensitive to a variety of protein-specific reagents. Together, these results are consistent with a mechanism for long-chain FA transport across red cell membranes that does not require protein-mediation and probably involves translocation across the lipid phase of the membrane.

Comparison with Previous Studies. Previous studies from which information was obtained about FA transport across red cells involved measurements of the uptake and extraction of radiolabeled FA. In the first detailed investigation of FA uptake in red cells, evidence was obtained for an energy-dependent step in which a fraction of the cell-associated FA

could not be extracted by albumin (*29*). This raised the possibility that movement of FA through the cell membrane might be energy-dependent. In contrast, a study of both intact red cells and ghosts found that all of the cell-associated FA could be extracted by incubation with albumin (*31*). Moreover, in this study cells were treated with a variety of protein-modifying reagents, none of which had an effect on the rate of FA uptake, and it was found that the half-time of oleate translocation at 4 °C was less than 15 s. Finally, in a series of studies, Bojesen and Bojesen (*32*−*36*) investigated in considerable detail the binding and kinetics of FA uptake and efflux in human red cells. They found that binding of FA to red cell ghosts involves a discrete number of sites that constitute about 1% of the phospholipid concentration and are distributed asymmetrically in the inner and outer halves of the bilayer, and the number and distribution of these sites are different for different FA. These results led to the conclusion that transport of FA occurs through lipid microdomains that are delineated by proteins and that these domains are different for palmitate, oleate, and arachidonate (*35*, *36*).

Results of the present study indicate that FA binding to red cell ghosts is governed by a lipid/aqueous partition mechanism rather than one involving a relatively small (1% of phospholipid) number of sites. Thus, our results indicate that amounts of FA in excess of 40 mol% can bind and that K_p values are independent of the fraction of FA bound to ghosts (Table 1, Methods). Moreover, the variation of K_p with FA type is consistent with partition of FA between aqueous and hydrocarbon phases, reflecting the dominant influence of FA solubility in this process, and in particular the K_p values obtained for red cell ghosts (Table 1) are virtually identical to those for lipid vesicles (*44*, *45*). Thus, our results are not consistent with binding characteristics suggesting that transport across the red cell membranes occurs within FA-specific domains. On the other hand, quite similar half-times (20−30 s) for transport of oleate and palmitate were obtained by both Bröring et al. (*31*) and Bojesen and Bojesen (*32*), respectively, and these values are consistent with the values from the present study when extrapolated to the 0−4 °C temperature range. In addition, our results indicating that the rate of linoleate transport across ghosts as well as lipid vesicles is greater (≥3-fold) than palmitate or oleate (*27*) are consistent with a similar trend found for arachidonate, relative to palmitate and oleate, by Bojesen and Bojesen (*32*). Our results also indicate that transport across ghost membranes is energy-independent because time courses were not significantly different for ghosts trapped with ATP, KCl/glucose, or with the standard NaCl buffer (A) without glucose (data not shown). Transport rates were also independent of [unbound FFA] for concentrations ranging from normal physiologic levels (<10 nM) to greater than 1000 nM. Finally, although k_{ff} and k_{off} for ghosts are 2−3-fold larger than for egg phosphatidylcholine−cholesterol vesicles (*27*), the behavior with temperature and FA type are virtually identical to these lipid vesicles. This difference in rates might reflect the more complex lipid environment of the ghost membrane and/or the modification of lipid properties by membrane proteins. Thus, although not excluding participation of protein components, the present results are similar to those obtained for lipid vesicles and are consistent with the conclusions of Bröring et al. (*31*) that FA transport across the red cell membrane is most simply described as a lipid-mediated process.

Table 5: Eyring Rate Theory Analysis of the Flip-Flop Rate Constants[a]

fatty acid	$\Delta G^{\ddagger\circ}$	$\Delta H^{\ddagger\circ}$	$-T\Delta S^{\ddagger\circ}$
oleate	18.1	7	12
palmitate	18.1	7	11
linoleate	17.3	7	10

[a] Values for the activation thermodynamic parameters $\Delta G^{\ddagger\circ}$, $\Delta H^{\ddagger\circ}$, and $-T\Delta S^{\ddagger\circ}$ are in kilocalories per mole and were determined from the k_{ff} values of Table 4 using the Eyring rate theory as described previously (*19*, *22*). Uncertainties for $\Delta G^{\ddagger\circ}$ are about 0.1 kcal/mol and about 2 kcal/mol for $\Delta H^{\ddagger\circ}$ and $-T\Delta S^{\ddagger\circ}$.

Relevance for Understanding Mechanisms of Long-Chain FA Translocation across Membranes. Although these results are consistent with transport of long-chain FA across red cell membranes as mediated by interactions similar to those involved in transport across lipid bilayers, the mechanism of transbilayer translocation remains unclear. In particular, whether it is appropriate to describe flip-flop of FA across the lipid phase of membranes as governed by simple diffusion requires clarification. For example, if flip-flop were mediated by the same interactions that govern lateral diffusion of membrane lipids, then using $D \sim 1 \times 10^{-8}$ cm^2/s (*48*, *49*), flip-flop times should be about 4×10^{-6} s or more than 5 orders of magnitude faster than the >1 s observed in the present study and in (*27*). Previous studies of the permeability of a variety of nonelectrolytes through lipid bilayers have noted similar discrepancies, which suggest that transmembrane translocation may be better described as diffusion through a polymer of fairly high tortuosity than by diffusion through an oil of viscosity equal to 1 P, a value which is consistent with rates of lateral diffusion (*50*). Further insight into the nature of the barrier to flip-flop is provided by an Eyring rate theory analysis which reveals similar activation enthalpies (∼7 kcal/mol) for all three FA, with a nominally lower entropic barrier for linoleate accounting for its lower activation free energy (Table 5). These results are similar to those obtained previously for lipid vesicles (*27*), although with somewhat lower $\Delta H^{\ddagger\circ}$ values and correspondingly larger entropic contributions. These entropic contributions for native FA are, however, about 8 kcal/mol lower than those for the anthroyloxy FA, raising the possibility that the entropic contributions of the barrier reflect the tortuosity of the membrane, with the more bulky anthroyloxy FA experiencing much larger barriers than the native FA and, possibly, the red cell ghost membrane exhibiting a somewhat higher degree of tortuosity than the lipid vesicles.

This issue of the mechanism by which FA cross lipid and ghost membranes is relevant to cellular transport because if a lipid bilayer's barrier to flip-flop is substantial, more complex biological membranes, especially in cells for which FA metabolism is a central function, may require protein-mediated mechanisms to achieve the necessary levels of FA metabolism. For example, as discussed previously, transport rates across cardiac myocyte membranes might have to be faster than in lipid vesicles or ghosts to support observed rates of FA metabolism (*27*). However, using the same methods for estimating the required transport rates in red cells and a value of 30 nmol^{-1} hr (ml of packed red cells)$^{-1}$

(*29*), we estimate that the transport rate constant necessary to support this metabolic rate for palmitate is $\geq 3.5 \times 10^{-3}$ s^{-1}. This value is about 300-fold smaller than the observed rate constants in ghosts or lipid vesicles and suggests that a protein-mediated mechanism is not required in red cells.

REFERENCES

1. Abumrad, N. A., Perkins, R. C., Park, J. H., and Park, C. R. (1981) *J. Biol. Chem. 256*, 9183−9191.
2. Schwieterman, W., Sorrentino, D., Potter, B. J., Rand, J., Kiang, C. L., Stump, D., and Berk, P. D. (1988) *Proc. Natl. Acad. Sci. U.S.A. 85*, 359−363.
3. Sorrentino, D., Robinson, R. B., Kiang, C.-L., and Berk, P. D. (1989) *J. Clin. Invest. 84*, 1325−1333.
4. Berk, P. D., Wada, H., Horio, Y., Potter, B., Sorrentino, D., Zhou, S. L., Isola, L., Stump, D., Kiang, C. L., and Thung, S. (1990) *Proc. Natl. Acad. Sci USA 87*, 3484−3488.
5. Harmon, C. M., Luce, P., Beth, A. H., and Abumrad, N. A. (1991) *J. Membr. Biol. 121*, 261−268.
6. Kumar, G. B., and Black, P. N. (1993) *J. Biol. Chem. 268*, 15469−15476.
7. Abumrad, N. A., El-mmaghrabi, M. R., Amri, E., Lopez, E., and Grimaldi, P. A. (1993) *J. Biol. Chem. 268*, 17665−17668.
8. Stremmel, W., Kleinert, H., Fitscher, B., Gunawan, J., Klaassen-Schlüter, C., Möller, K., and Wegener, M. (1992) *Biochem. Soc. Trans. 20*, 814−817.
9. Schaffer, J. E., and Lodish, H. F. (1994) *Cell 79*, 427−436.
10. Trigatti, B. L., Mangroo, D., and Gerber, G. E. (1991) *J. Biol. Chem. 266*, 22621−22625.
11. Fujii, S., Kawaguchi, H., and Yasuda, H. (1987) *Lipids 22*, 544−546.
12. Faergeman, N. J., DiRusso, C. C., Elberger, A., Knudsen, J., and Black, P. N. (1997) *J. Biol. Chem. 272*, 8531−8538.
13. Cooper, R. B., Noy, N., and Zakim, D. (1989) *J. Lipid Res. 30*, 1719−1726.
14. Meddings, J. B., and Dietschy, J. M. (1989) *J. Lipid Res. 30*, 1289−1296.
15. Kamp, F., Westerhoff, H. V., and Hamilton, J. A. (1993) *Biochemistry 32*, 11074−11086.
16. Hamilton, J. A., Civelek, V. N., Kamp, F., Tornheim, K., and Corkey, B. E. (1994) *J. Biol. Chem. 269*, 20852−20856.
17. Kamp, F., Zakim, D., Zhang, F., Noy, N., and Hamilton, J. A. (1995) *Biochemistry 34*, 11928−11937.
18. Civelek, V. N., Hamilton, J. A., Tornheim, K., Kelly, K. L., and Corkey, B. E. (1996) *Proc. Natl. Acad. Sci. U.S.A. 93*, 10139−10144.
19. Doody, M. C., Pownall, H. J., Kao, Y. J., and Smith, L. C. (1980) *Biochemistry 19*, 108−116.
20. Daniels, C., Noy, N., and Zakim, D. (1985) *Biochemistry 24*, 3286−3292.
21. Storch, J., and Kleinfeld, A. M. (1986) *Biochemistry 25*, 1717−1726.
22. Kleinfeld, A. M., and Storch, J. (1993) *Biochemistry 32*, 2053−2061.
23. Kleinfeld, A. M., Chu, P., and Storch, J. (1997) *Biochemistry 36*, 5702−5711.
24. Srivastava, A., Singh, S., and Krishnamoorthy, G. (1995) *J. Phys. Chem. 99*, 11302−11305.
25. Richieri, G. V., Ogata, R. T., and Kleinfeld, A. M. (1992) *J. Biol. Chem. 267*, 23495−23501.
26. Richieri, G. V., Ogata, R. T., and Kleinfeld, A. M. (1996) *J. Biol. Chem. 271*, 11291−11300.
27. Kleinfeld, A. M., Chu, P., and Romero, C. (1997) *Biochemistry 36*, 14146−14158.
28. Oliveira, M. M., and Vaughn, M. (1964) *J. Lipid Res. 5*, 156.
29. Shohet, S. B., Nathan, D. C., and Karnovsky, M. L. (1968) *J. Clin. Invest. 47*, 1096−1108.
30. Morand, O., and Aigrot, S. (1985) *Biochim. Biophys. Acta 835*, 68−76.
31. Broring, K., Haest, C. W. M., and Deuticke, B. (1989) *Biochim. Biophys. Acta 986*, 321−331.
32. Bojesen, I. N., and Bojesen, E. (1990) *Mol. Cell. Biochem. 98*, 209−215.
33. Bojesen, I. N., and Bojesen, E. (1991) *Biochim. Biophys. Acta 2736*, 297−307.
34. Bojesen, I. N., and Bojeesen, E. (1992) *Biochim. Biophys. Acta 2736*, 185−196.
35. Bojesen, I. N., and Bojesen, E. (1996) *Acta. Physiol. Scand. 156*, 501−516.
36. Bojesen, I. N., and Bojesen, E. (1996) *J. Membr. Biol. 149*, 257−267.
37. Dodge, J. T., Mitchell, C., and Hanahan, D. J. (1963) *Arch. Biochim. Biophys. 100*, 119−130.
38. Schwoch, G., and Passow, H. (1973) *Mol. Cell. Biochem. 2*, 197−218.
39. Gomori, G. (1942) *J. Lab. Clin. Med. 27*, 955−960.
40. Richieri, G. V., and Kleinfeld, A. M. (1995) *J. Lipid Res. 36*, 229−240.
41. Richieri, G. V., Anel, A., and Kleinfeld, A. M. (1993) *Biochemistry 32*, 7574−7580.
42. Weisiger, R. A., and Ma, W. L. (1987) *J. Clin. Invest. 79*, 1070−1077.
43. Richieri, G. V., Ogata, R. T., and Kleinfeld, A. M. (1996) *J. Biol. Chem. 271*, 31068−31075.
44. Anel, A., Richieri, G. V., and Kleinfeld, A. M. (1993) *Biochemistry 32*, 530−536.
45. Richieri, G. V., Ogata, R. T., and Kleinfeld, A. M. (1995) *J. Biol. Chem. 270*, 15076−15084.
46. Kleinfeld, A. M., and Chu, P. (1993) *Biophys. J. 64*, A306.
47. Kleinfeld, A. M. (1995) in *Stability and permeability of lipid bilayers* (Disalvo, E. A., and Simon, S., Eds.) pp 241−258, CRC Press, Boca Raton.
48. Edidin, M. (1974) *Annu. Rev. Biophys. Bioeng. 9038*, 180−201.
49. Wolf, D. E., Schlessinger, J., Elson, E. L., Webb, W. W., Blumenthal, R., and Henkart, P. (1977) *Biochemistry 16*, 3476−3483.
50. Stein, W. D. (1986) *Transport and diffusion across cell membranes*, Academic Press, Inc., Orlando.

BI980301+